EXPERIMENTAL STUDY OF THE MORPHING FLAP AS A LOW NOISE HIGH LIFT DEVICE FOR AIRCRAFT WING

Yasuhiro TANI*, Yoshiyuki MATSUDA*, Akira DOI*, Yuya YAMASHITA*, Shigeru ASO*, Takeshi ITO**

*** Department of Aeronautics and Astronautics, Kyushu University, Fukuoka, Japan,**

**** Wind Tunnel Technology Center, Japan Aerospace Exploration Agency, Tokyo, Japan**

tani@aero.kyushu-u.ac.jp; m-yoshiyuki@aero.kyushu-u.ac.jp; a_doi@aero.kyushu-u.ac.jp; Yu.Yama@aero.kyushu-u.ac.jp; aso@aero.kyushu-u.ac.jp; ito@chofu.jaxa.jp

Keywords: *morphing flap, high lift device, noise, wind tunnel test*

Abstract

To reduce the aeroacoustic noise of wings with high lift devices, a morphing flap configuration was proposed, which has smoothly contoured flap connected smoothly to the outer main wing. An wind tunnel test for NACA23012 wing model with interchangeable slotted flap was conducted in Kyushu university 2m x 2m Low-speed low-noise wind tunnel, at the condition of U=10 to 25m/s, Re=3.1 to 7.7x10^5. Flap configurations tested were single slotted flap with deflection angle of 0 to 20 degrees and a morphing flap with deflection angle of 30 degrees at flap root smoothly contoured to 0 degree at flap edge section. Aeroacoustic noise was measured using phased array microphones and analyzed by the beamforming method. The measured results showed that the morphing flap has capability to suppress the flap side-edge noise and reduce the overall sound pressure level.

1 Introduction

Recently, environmental issue is one of the most important problems to be improved for the future growth of the air transportation system. The attention has focused on the reduction of aircraft noise near the airport during take-off and landing. In these days, the noise from the propulsion system has been reduced considerably and it is of the same order of airframe noise at landing phase[1]. Therefore it is required to reduce airframe noise for the realization of quiet aircrafts. Major sources of the airframe noise at landing are the landing gear systems, turbulent boundary layer flow over the wings and fuselage, and flow around the high lift devices[2].

In this study, we focused on the flap side-edge noise for the slotted flaps, which is caused by the vortex flow around the flap side-edge. Various concept have been evaluated to reduce the flap side-edge noise. But there is a limit to the noise reduction effect of addition of small devices to the flap side-edge, such as fences, micro tabs, brush or porous surface. One of the promising method is the continuous moldline (CML) flaps, which has a small fairing between the main wing trailing edge and flap trailing edge to eliminate the flap side edge, and it has been reported that CML flaps can reduce the noise level at the flap side-edge[3]. However, this type configuration has span wise lift change between inner flap section and outer wing section, and it causes the increase of the induced drag.

The authors have been investigated on the morphing wings which changes the wing shape; airfoil cross section shape, planform, and so on [4][5]. As an application of this morphing wing concept, we applied it to the high lift devices to reduce not only the airframe noise but also aerodynamic drag. In this paper, wind tunnel test results are introduced to examine the effect of the morphing flap with smooth span wise flap deflection distribution on the noise reduction by means of noise source survey using phased array microphone system.

2 Experimental Setup

2.1 Wind Tunnel Test Facility

Wind tunnel test was conducted at the Low-speed low-noise wind tunnel in Department of Aeronautics and astronautics, Kyushu university, shown in figure 1. This wind tunnel is a closed circuit and has two test sections, a closed test section and a open type test section. In this experiment, we used the open type No.1 test section shown in figure 2, whose dimension is 2m x 2m octagonal and 5 m length in an anechoic chamber. Maximum velocity is 60 m/s and noise level is 65 dB at 40 m/s.

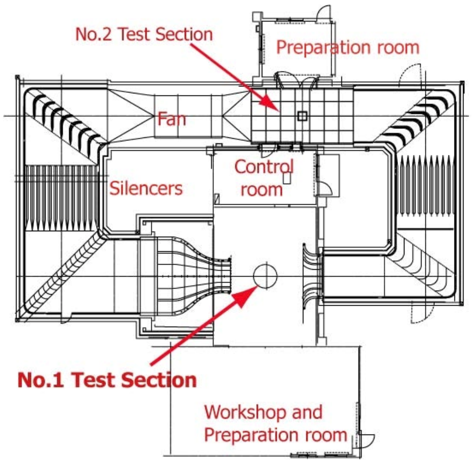

Fig. 1. Overview of Low-speed low-noise wind tunnel in Kyushu university

Fig. 2. No.1 low-noise test section

2.2 Wind Tunnel Test Model

The test model is a half span wing model with 1150 mm width and 450 mm chord length, whose cross section is NACA23012. At the trailing edge of the inner half span region of the wing, two types of interchangeable high lift devices were installed. One is a conventional single slotted flap, and another is a morphing flap, with flap chord length of 40%c of the base wing. For the single slotted flap configuration, flap deflection angle can be set as 0, 10, 20 degrees. Morphing flap configuration has smoothly changing distribution in deflection angle and fowler motion in span wise. Cross section at 50% span location is smoothly connected from inner to outer wing. Deflection angle at wing root section was set as relatively large at the wing root, to account the lift loss at outer part of the morphing flap. Consequently, deflection angle distribution was set as 30 degrees at flap root section and 0 degree at flap edge section, and the average deflection angle was 15 degrees.

This half wing model was supported on a half body model, which has function as a wind shield of force balance and a simplified aircraft fuselage, placed on the wind tunnel lower wall

Figure 3 shows the conceptual sketch and the wind tunnel test model of morphing flap configuration. Figure 4 shows the model installation in the wind tunnel test section.

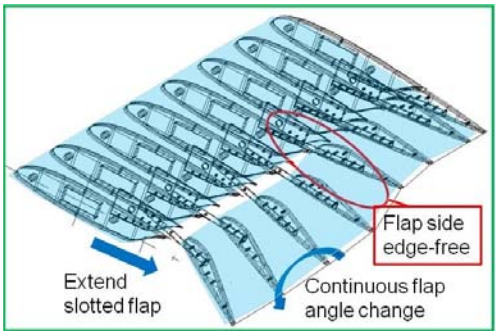

(a) Conceptual sketch of morphing flap

(b) Upper view of test model (morphing flap)

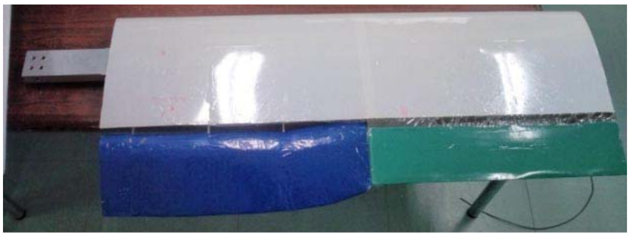

(c) Rear view of test model (morphing flap)

Fig. 3. Morphing flap concept and wind tunnel test model

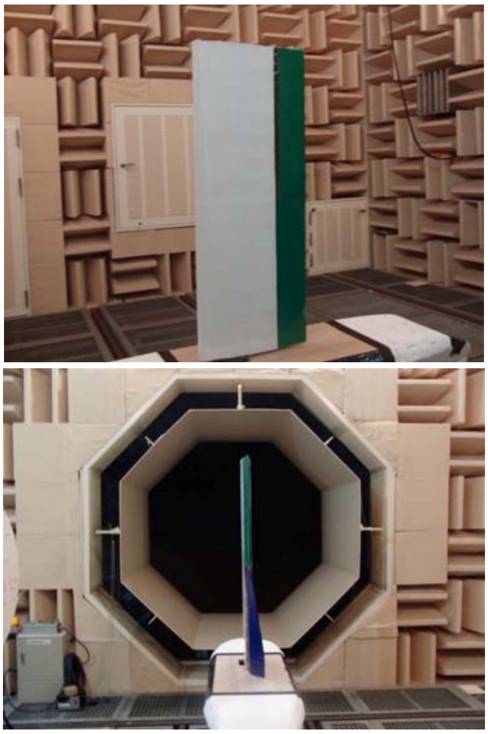

Fig. 4. Model installation in wind tunnel test section

2.3 Measurements and Test Conditions

Six component aerodynamic forces and moments were measured using a force balance (Nissho electric works LMC-6524) mounted on the lower wall of wind tunnel test section, and the wing model was fixed on the force balance.

Noise source survey measurement was carried out using a phased array microphone system. This measurement system was developed by Wind Tunnel Technology Center (WINTEC) of Aerospace Research and Development Directorate (ARD) of Japan Aerospace Exploration Agency (JAXA), and modified to fit to the wind tunnel in Kyushu university.

This microphone array system consisted of 32 microphones (G.R.A.S. Type 40PH), two data acquisition modules (National Instruments PXI-4498) and a PC. The microphones have diameter of 7 mm, their frequency range of 10 Hz to 20 kHz and their dynamic range of 32 dB to 135 dB, and each has an integrated preamplifier in it. The A/D converter has 24 bit resolution, up to 114 dB dynamic range and simultaneous sampling on all channels at rates up to 204.8 kSamples/s.

Multi-arm-spiral arrangement of the microphones was applied for the array design. Microphones were set on a polystyrene form board to fix position and to be able to change it easily. The heads of the microphones extended out through the polystyrene board surface to reduce the effect of the sound reflection at the board surface. The location of the microphone array was just beside 1500 mm from the wing model. The arrangement of the microphone array to be used in this wind tunnel test was shown in figure 5 and 6. Diameter of the array was 1000 mm considering the measurement frequency up to 6 kHz. Data processing method used in this study was delay-and-sum beamforming method.

Besides the noise source survey, the overall sound pressure level (SPL) was measured using a sound field microphone (RION UC-31) with a preamplifier (RION NH-04A) and a multi channel signal analyzer (RION SA-01). Frequency range of the microphone is 10 Hz to 35 kHz and frequency range of the preamplifier is 10 Hz to 100 kHz. Figure 7 shows the measurement system and model setup in the wind tunnel.

Test condition was selected as follows; flow velocity U was ranged from 10 to 25 m/s, angle of attack α was 0 to 20 degrees, and flap deflection angle δ_f was 0, 10 and 20 degrees for the single slotted flap. Flap angle distribution for the morphing flap was set as 30 degrees at the root and changed smoothly to 0 degree at the flap tip shown in figure.3. Reynolds number based on the wing chord length was Re=3.1×10^5 to 7.7×10^5.

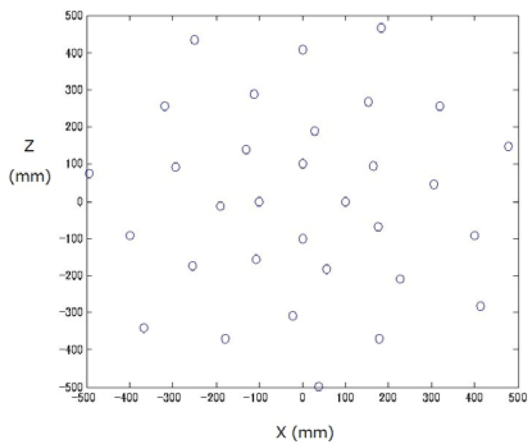

Fig. 5. Multi-arm-spiral microphone arrangement

Fig. 6. Microphone array and microphone installation

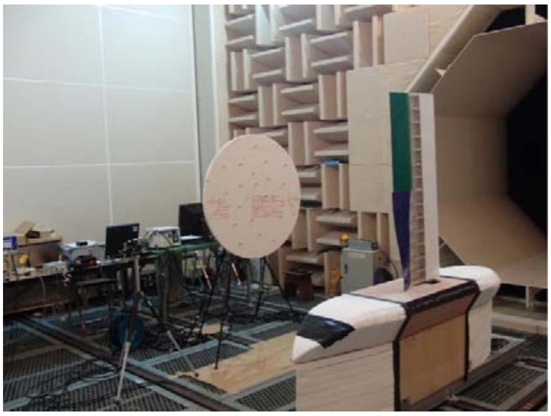

Fig. 7. Measurement setup in the test section

3 Results and Discussions

3.1 Speaker Test Results

At first, to confirm the aeroacoustic noise measurement system, a small audio speaker was tested in the test section as a point sound source. Center coordinates of the speaker was x=200mm and z=-460mm. Figure 8 shows the noise source survey visualization results. Because of the microphone array diameter, noise source is not clear for the low frequency sound source, but it can be clearly detected for high frequency. This results show the noise source survey results were reasonable and showed the detectability of the measurement system used in this study.

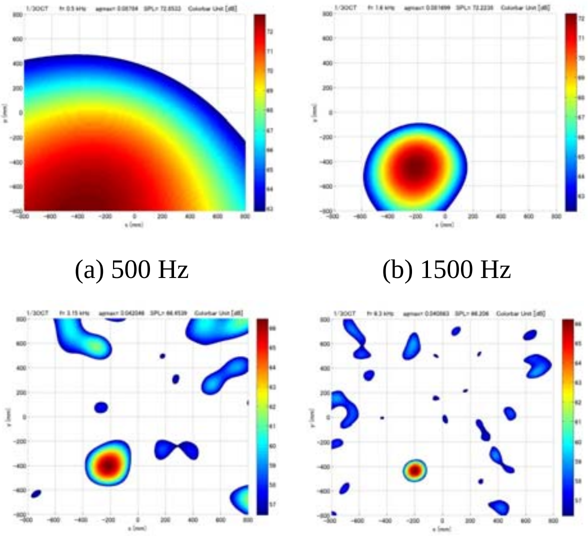

(a) 500 Hz (b) 1500 Hz

(c) 3000 Hz (d) 6000Hz

Fig. 8. Noise source survey for speaker test

3.2 Morphing Flap Model Test Results

Figure 9 shows the comparison of SPL and figure 10 to 12 show the comparison of noise survey results at U=20 m/s and angle of attack 0 degree, for four configurations; δ_f =0, 10 and 20 degrees of the single slotted flap and the morphing flap. As shown in figure 9, morphing flap has almost same noise level at low frequency but lower at high frequency compared with the single slotted flap case.

Figure 10 to 12 shows the noise survey results for the three frequency; 1250, 2500, 5000 Hz respectively. This figure shows that the noise source at the wing root was remarkable for single slotted flap of δ_f =20 degree and morphing flap. This noise source is seemed to be caused by the flow separation at the wing root for large flap deflection angle. Noise source at the flap side-edge was observed for δ_f =10 and 20 degrees single slotted flap in figure 11 and 12, and clear noise source was observed for δ_f =20 degree flap especially for the 5000 Hz. In compared with this, it was not observed for the morphing flap.

Figure 13 shows the comparison of SPL and figure 14 to 16 show the comparison of noise survey results at U=20 m/s and angle of attack 5 degrees. Figure 14 to 16 show the comparison of noise survey results for the three frequency; 1250, 2500, 6300 Hz, and four flap configurations. As larger angle of attack, noise source area became large for low frequency for all the configurations, because of flow disturbance and turbulence. For 6300Hz, noise source at flap side-edge single slotted flap was observed more clearly than that of α=0 degree. However, noise source around the flap edge was not observed for morphing flap. As this morphing flap configuration has continuous cross sectional shape change, there are continuous span wise flow field distribution around the wing. Therefore, the morphing flap could suppress the aeroacoustic noise.

Figure 17 shows the comparison of the overall pressure level for all the cases. For single slotted flap configurations, overall pressure level increases as velocity, angle of attack and flap deflection angle basically. Overall pressure level of the morphing wing shows between δ_f =10 and 20 degrees of single slotted flap for almost all the cases, and this shows the capability of the morphing flap to reduce the aeroacoustic noise. As for U=10m/s, tendency of strength of overall pressure is different from other velocity cases. Because the flow Reynolds number is small, boundary layer transition might account for this phenomena.

From the wind tunnel test results, morphing flap showed lower noise level in high frequency and suppress the noise source at flap side-edge region. But the noise source caused by the flow separation at wing root and at low frequency decreases the noise reduction effect of the morphing flap.

In this study, one morphing flap configuration was compared with single slotted flap configurations. But its cross section shape distribution can be set freely to suppress the flow separation around the wing root. Therefore it is probable that the morphing flap will achieve the reduction of noise level at wide frequency range.

4 Conclusions

Low speed wind tunnel test was conducted to examine the noise reduction effect of morphing flap. Noise source survey measurement using microphone array and beamforming method showed that flap side-edge noise can be reduced by the morphing flap for the half span wing model. The results lead to the conclusion that there is the possibility to realize the low noise high lift device with morphing wing concept, and further investigation is required for precise evaluation.

Acknowledgement

This work was supported by MEXT/JSPS KAKENHI Grant Number(23560956).

References

[1] Dobrzynski, Almost 40 years of airframe noise research: what did we achieve?, *Journal of aircraft*, Vol. 47 No.2, pp.353-367, 2010.

[2] Streett, C. L., Numerical simulation of a flap-edge flowfield, AIAA-98-2226, 1998.

[3] Streett, C. L., et. al., Aerodynamic noise reduction for high-lift devices on a swept wing model, AIAA-2006-212, 2006.

[4] Tani, Y., Yayama, T., Hashimoto J. and Aso, S., Conceptual design of ecological aircraft for commuter air transportation, ICAS 2008-1.2.3, 2008.

[5] Tani, Y., Doi, A., Aso, S., Hashimoto J., A conceptual study of electric small aircraft with morphing wing, *Proceedings of the 48th aircraft symposium*, JSASS-201-05119, 2010.

[6] Ito, T., Ura, H. et.al., Aerodynamic/aeroacoustic testing in anechoic closed test sections of low-speed wind tunnels, AIAA 2010-3750, 2010.

[7] Mueller, Thomas J.(Ed.). *Aeroacoustic measurement*, Springer, 2001.

Copyright Statement

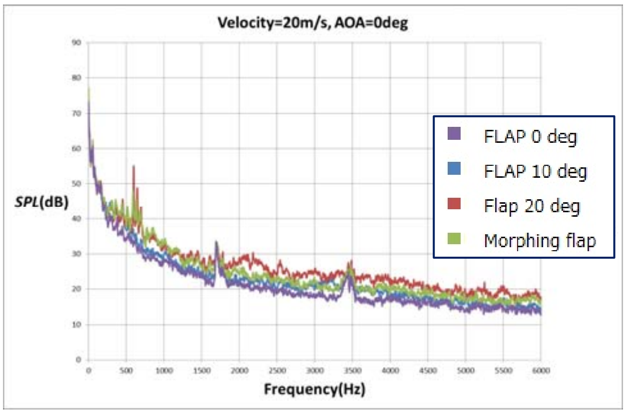

Fig. 9. SPL : U=20m/s, α=0 deg

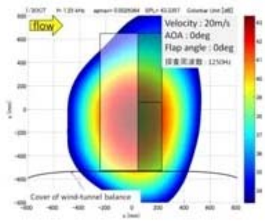

(a) Flap 0 deg

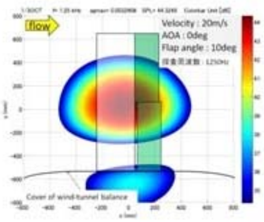

(b) Flap 10 deg

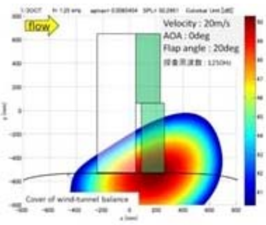

(c) Flap 20 deg

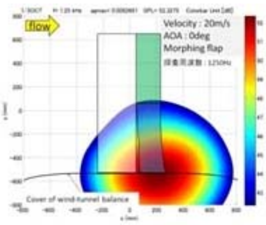

(d) Morphing flap

Fig.10. U=20m/s, α=0 deg, *f*=1250Hz

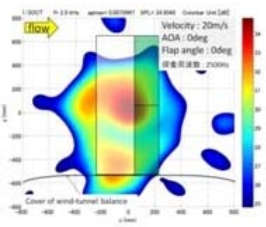

(a) Flap 0 deg

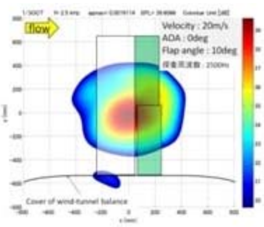

(b) Flap 10 deg

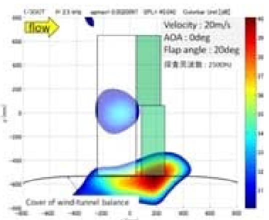

(c) Flap 20 deg

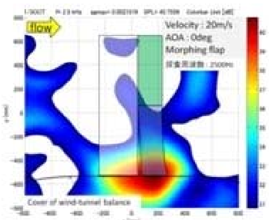

(d) Morphing flap

Fig.11. U=20m/s, α=0 deg, *f*=2500Hz

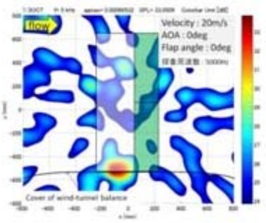

(a) Flap 0 deg

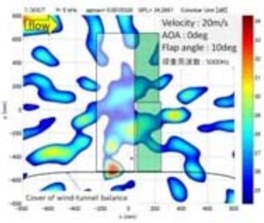

(b) Flap 10 deg

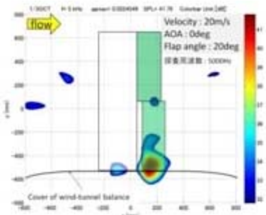

(c) Flap 20 deg

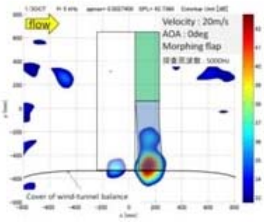

(d) Morphing flap

Fig.12. U=20m/s, α=0 deg, *f*=5000Hz

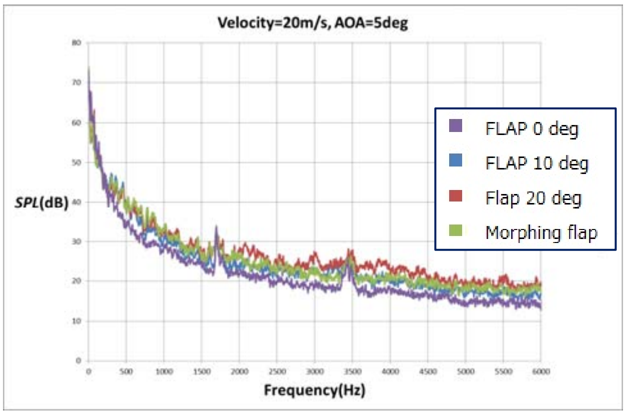

Fig. 13. SPL : U=20m/s, α=5 deg

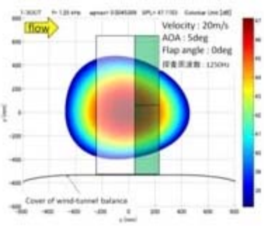

(a) Flap 0 deg

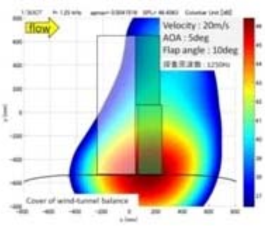

(b) Flap 10 deg

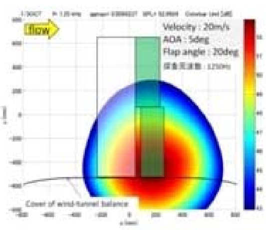

(c) Flap 20 deg

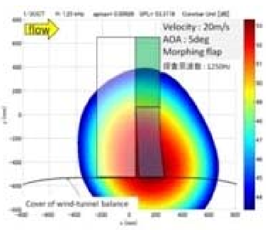

(d) Morphing flap

Fig.14. U=20m/s, α=5 deg, *f*=1250Hz

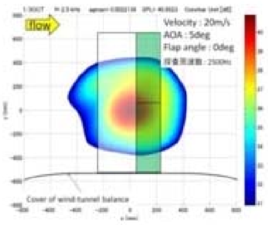

(a) Flap 0 deg

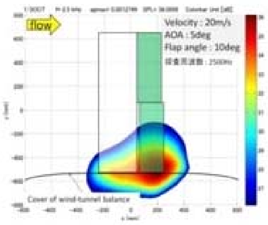

(b) Flap 10 deg

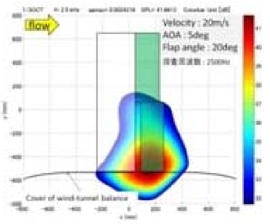

(c) Flap 20 deg

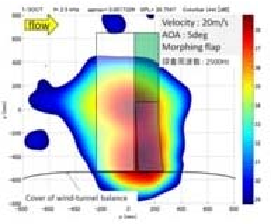

(d) Morphing flap

Fig.15. U=20m/s, α=5 deg, f=2500Hz

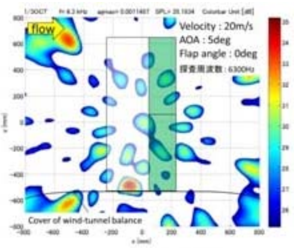

(a) Flap 0 deg

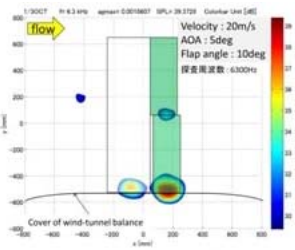

(b) Flap 10 deg

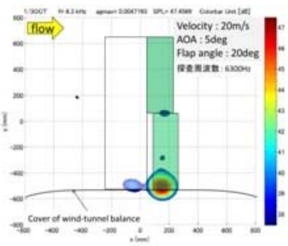

(c) Flap 20 deg

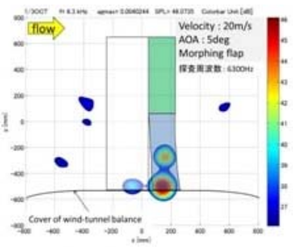

(d) Morphing flap

Fig.16. U=20m/s, α=5 deg, f=6300Hz

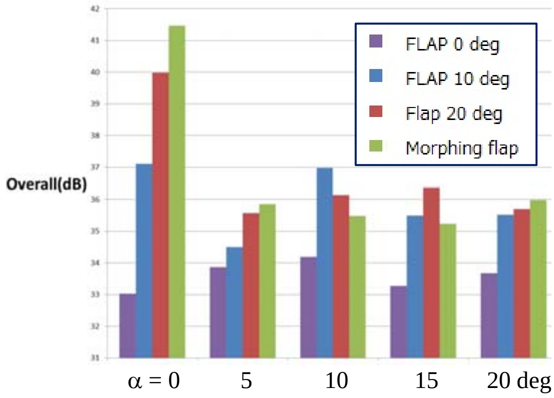

(a) U = 10 m/s

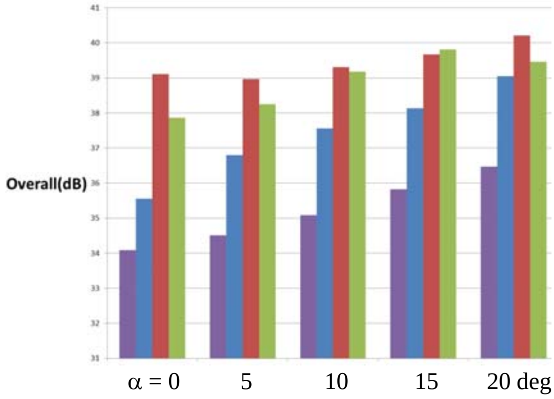

(b) U = 20 m/s

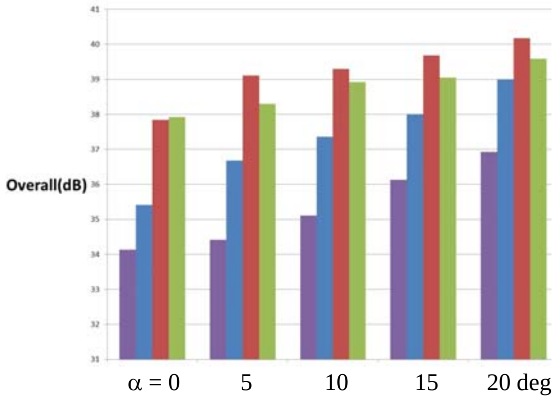

(c) U = 25 m/s

Fig. 17. Comparison of overall pressure level